Synthetic Metals 237 (2018) 56–64

Contents lists available at ScienceDirect

Synthetic Metals

journal homepage: www.elsevier.com/locate/synmet

Development of an improved synthetic route to triply linked di(perylene bisimides) with varied substituents and their performance as non-fullerene acceptors in polymer photovoltaics

Levi M.J. Moore, Mark B. Norman, Anthony R. Benasco, Julian M. Richardson, Sarah E. Morgan*

The University of Southern Mississippi, School of Polymer Science and Engineering, 118 College Drive, #5050, Hattiesburg, MS 39406, United States

ARTICLE INFO

Keywords:
Perylene bisimide dimers
Polymer photovoltaics
Non-fullerene acceptors
Atomic force microscopy

ABSTRACT

A series of triply-linked perylene bisimide dimers (diPBIs) with varied solubilizing groups (short-chain aliphatic, long-chain aliphatic, and aryl) were synthesized to determine the structure-property relationships that govern their performance as non-fullerene acceptors in conventional polymer photovoltaic devices. In the synthesis of the intermediates, a new solvent and ligand system for dehalogenation of 1,6,7,12-tetrabromo-perylene bisimides to 1,12 dibromo-perylene bisimides was developed in order to access PBI systems that are not available via procedures previously reported. The new dimethylacetamide/2-picolinic acid system expands the available R-groups for inclusion on perylene bisimides that render them insoluble in the conventional DMSO/L-proline system, while providing milder conditions and higher yields. A cosolvent system of DMSO/diphenyl sulfoxide was utilized to couple the brominated perylene bisimides, allowing for direct coupling of aliphatic-substituted perylene bisimides. The resulting diPBIs showed only very small differences in optoelectronic properties, but aliphatic-substituted diPBIs provided better performance due to their better solubility and ability to form co-continuous films with the donor polymer PTB7.

1. Introduction

In recent years, polymer photovoltaics have shown much promise as part of the renewable energy landscape, specifically by making photovoltaics more accessible through mass production like blade coating or inkjet printing. The majority of recent research on new materials has focused on the donor polymer of the device rather than the electron acceptor material. However, lately there has been increased interest in alternative, non-fullerene acceptor materials to replace compounds like phenyl-C_{61}-butyric acid methyl ester (PCBM) [1–3]. An intriguing class of materials for this application is based on perylene bisimide, (PBI), an industrially important colorfast dye that has seen utility in the organic electronics area from the beginning of organic photovoltaics, a derivative of which was utilized in the first organic photovoltaic device [4] due to its chemical tunability, high electron mobility, and environmental stability [5–7]. Due to these advantageous factors, PBIs have been widely utilized as the electron accepting material in organic solar cells, both as small molecules and incorporated into polymers [8–10]. The identity of the imide R group affects the solubility and self-assembly characteristics of PBIs, leading to varied optoelectronic properties once solution cast into the solid state [11]. Expanding the conjugation of the bay region of the PBI through addition of phenyl groups [12] or additional PBI moieties [6,13–15] has been one approach to broaden the absorption and tune the electronic properties of PBI-based molecules [12]. One promising approach is to expand the bay region through linkage of the PBI to another PBI through three bonds, in contrast to one or two.

A variety of these types of compounds have been synthesized, all using the method of copper-mediated Ullmann-style coupling, with CuI as the copper source, L-proline as the ligand, and DMSO as the solvent. CuI/L-proline is a well-studied system that has been widely used [16–18], notably in the coupling of aryl halides [19], and for reactions such as oxidation of alcohols to ketones [20]. Synthesis of triply-linked PBI dimers has been reported utilizing tetrahalogenated PBIs as the substrate for subsequent reaction either through direct coupling in basic conditions [21] or through synthesis of a 1,12-dihalogenated compound without addition of a base, which is then subjected to the same coupling conditions [22]. A few reports have appeared of the synthesis of these 1,12-dihalogenated compounds with either alkyl or aryl R-groups in the imide positions and either tetrachlorination or tetrabromination in the bay region. These studies all used DMSO as the solvent for their reactions with no reports of an alternative, limiting the applicability of

* Corresponding author.
E-mail address: sarah.morgan@usm.edu (S.E. Morgan).

https://doi.org/10.1016/j.synthmet.2018.02.005
Received 22 October 2017; Received in revised form 29 January 2018; Accepted 5 February 2018
Available online 10 February 2018
0379-6779/

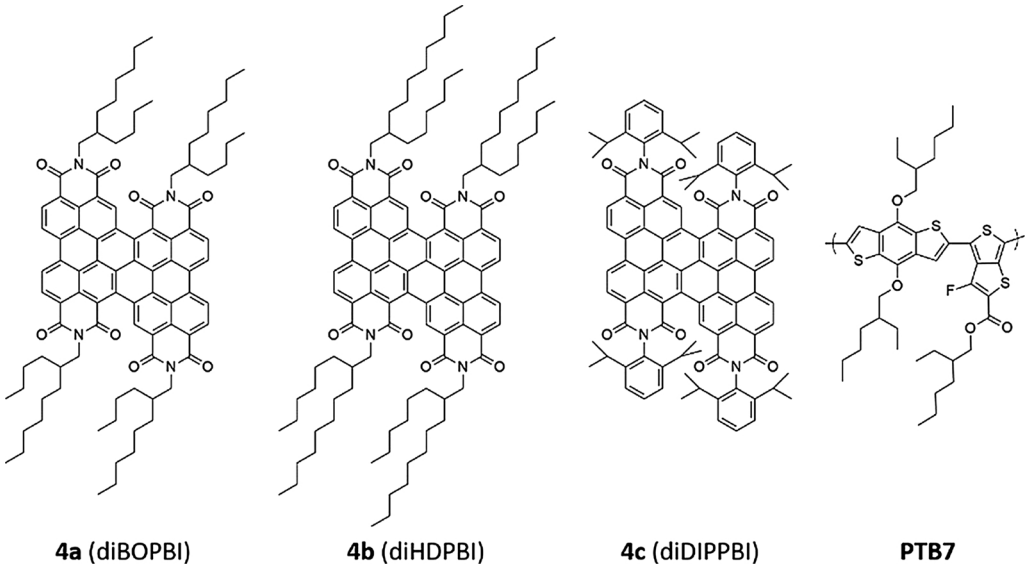

Fig. 1. Target diPBIs and polymer donor PTB7 used as polymer component in OPV devices.

these reaction conditions to only those functional groups soluble in DMSO. An alternative solvent system for the modification of these types of halogenated perylene bisimides is therefore desired to expand the range of architectures and structures possible for applicability in organic semiconductor research.

In this report, we detail the synthesis of a series of triply-linked perylene bisimide dimers (diPBIs) using intermediates synthesized under alternative milder conditions and in higher yields compared to previous reports of similar molecules. DiPBIs with three different solubilizing groups were synthesized: short chain alkyl (di(butyloctyl)PBI, diBOPBI, (4a), long chain alkyl (di(hexyldecyl)PBI, diHDPBI, (4b), and aryl (di(diisopropylphenyl)PBI, diDIPPBI, (4c). The aryl-substituted diDIPPBI has been synthesized in a previous publication,[21] but not yet reported in photovoltaic devices. Similar alkyl-substituted diPBIs have been utilized as non-fullerene acceptors [22], but the effect of alkyl chain length on device performance was not studied. The compounds synthesized in this study were utilized as non-fullerene acceptor materials in the active layer of bulk heterojunction polymer solar cells, with the polymer PTB7 acting as the donor material (Fig. 1).

2. Results and discussion

2.1. Synthesis and characterization of diPBIs

The syntheses of all target diPBIs (**4a–c**) involve a multistep process (Scheme 1), first requiring the synthesis of the tetrabromo-perylene bisanhydride (**1**) and then the synthesis of the tetrabromo-perylene diimides (**2a–c**), procedures of which are widely reported and easily reproduced from the literature (condition *i*, Scheme 1) [12,23]. Direct coupling of compound **2c** using the reported procedures in DMSO (condition *ii*) yielded compound **4c** in yields comparable to literature [21]. Direct coupling of the aliphatic tetrabromo-PBIs **2a** and **b** was attempted using condition *ii*, but the compounds were insoluble in DMSO, the solvent of choice for this style of coupling [22,24], so a different solvent was needed. The coupling reactions were attempted using DMSO and either toluene or dioxane as a cosolvent, without success. Diphenyl sulfoxide was chosen as the cosolvent to maintain the sulfoxide functionality of DMSO while also lowering the polarity of the solvent mixture, effectively solubilizing the tetrabromo-PBIs at a 3:1 mass ratio of DMSO to DPSO (condition *iii*). Direct coupling of the aliphatic tetrabromo-PBIs provided yields lower than, but comparable to, direct coupling of the aryl diPBI in literature [21].

In an effort to obtain a higher yield of the target compounds **4a** and **b** from a single reaction, a method similar to Jiang et al.'s report [22] was first utilized to dehalogenate the tetrabromo-PBIs in one bay. The solvent system of 3:1 DMSO/DPSO was utilized (condition *v*), and yields lower than those reported resulted (Table 1), likely due to the poor solubility of the tetrabromo-PBIs at the reaction temperature, which was only a few degrees above the melting point of DPSO. Screening for alternate solvents showed that dimethyl acetamide solubilizes **2a** and **b**, but L-proline was not soluble. Due to its solubility in DMAc and high activity in other similar copper-mediated reactions [20], 2-picolinic acid (2PA) was chosen as a ligand [20]. Dehalogenation of the tetrabromo-PBIs was performed with the DMAc/2PA combination (condition *vi*), which doubled the yield of the dibromo-PBIs as compared to the DMSO/DPSO/L-proline system, as well as for the dehalogenation of **2c** in DMSO (condition *iv*). These yields are greater than those obtained in other reports on the dehalogenation of aliphatic tetrahalogenated PBIs [23,25,26], presumably due to the increased solubility of the tetrabromo-PBIs in DMAc compared to DMSO or DMSO/DPSO mixtures. Coupling of the dibromo-PBIs was attempted utilizing the DMAc/2PA system, though only trace amounts of the desired diPBIs were obtained [27]. The DMSO/DPSO/L-proline system (condition *iii*) was utilized to couple the dibromo-PBIs. The yields of the target compounds utilizing the two-step synthetic route were higher than those of the direct method, but the overall yields from the one-step direct coupling were higher when starting from the tetrabrominated PBIs.

UV–visible spectroscopy (Fig. 2) shows similar absorption profiles for each molecule, indicating that the different diPBIs' solubilizing groups do not strongly affect the absorption of the molecules in solution, with only slight differences between the three compounds. In contrast, when cast into thin films, the aliphatic diPBIs show similar absorption profiles while the aryl diDIPPBI shows a great change in the low-energy region, which we suggest is a change in crystalline packing upon film formation. The optical band gap, estimated by the absorption onset in solution, is the same for each diPBI (Table 2). The energy levels (HOMO and LUMO) are quite similar and lie close to the values for similar molecules reported in the literature. Reductive cyclic voltammograms of the diPBIs are shown in Fig. 3. All diPBIs show four reduction waves consistent with similar compounds reported in the literature.[22,28,29] Because of the very similar energy levels and light absorption, any performance differences when incorporated into the active layer can be attributed to the identity of the R-groups and their variable solubilities.

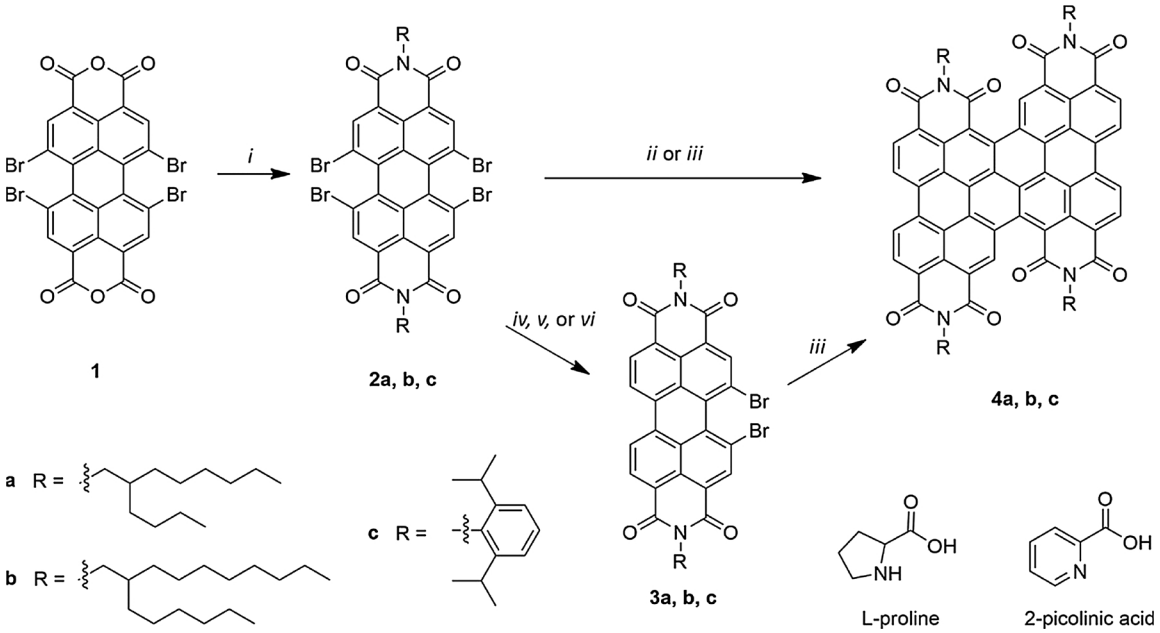

Scheme 1. Reaction scheme and conditions for the syntheses of diPBIs: i) R-NH_2, propionic acid, 140 °C, 4 h; ii) CuI, L-proline, K_2CO_3, DMSO, 110 °C, 12 h; iii) CuI, L-proline, K_2CO_3, DMSO/DPSO, 110 °C, 12 h; iv) CuI, L-proline, DMSO, 75 °C, 6 h; v) CuI, L-proline, DMSO/DPSO, 75 °C, 6 h; vi) CuI, 2-picolinic acid, dimethyl acetamide, 75 °C, 6 h.

Table 1
Reaction conditions and purified yields for target compounds. Values in parentheses represent overall yield when starting from the respective tetrabrominated precursor (**2a** or **2b**), calculated from the product of the purified yields from reaction conditions vi and iii from Scheme 1.

Target Compound	Reaction route	Yield (%)
Br_2BOPBI (**3a**)	DMSO/DPSO, L-proline (*v*)	23
	DMAc, 2PA (*vi*)	48
Br_2HDPBI (**3b**)	DMSO/DPSO, L-proline (*v*)	20
	DMAc, 2PA (*vi*)	46
Br_2DIPPBI (**3c**)	DMSO, L-proline (*iv*)	23
	DMAc, 2PA (*vi*)	50
diBOPBI (**4a**)	Two-step (*vi*, *iii*)	12 (6)
	Direct (*iii*)	10
diHDPBI (**4b**)	Two-step (*vi*, *iii*)	18 (8)
	Direct (*iii*)	10
diDIPPBI (**4c**)	Direct (*iii*)	25

Table 2
Photophysical properties of diPBIs in solution. λ_{onset} was calculated from the onset of absorption in dilute $CHCl_3$ solution (1×10^{-5} M), and E_g was calculated according to Eg (eV) = (1240 / λ_{onset}). E_{onset} was calculated from the onset of the reduction peak in cyclic voltammetry compared to the reduction peak of Fc/Fc^+ (Fig. 3). The LUMO of the diPBIs was estimated according to the onset of the reduction peaks and $E_{LUMO} = -(4.8 + E_{onset})$. The HOMO was calculated according to $E_{HOMO} = (E_{LUMO} - E_g)$ eV.

Compound	λ_{onset} (nm)	E_g (eV)	E_{onset} (V)	E_{LUMO} (eV)	E_{HOMO} (eV)
diBOPBI (**4a**)	701	1.77	−0.54	−4.26	−6.03
diHDPBI (**4b**)	702	1.77	−0.59	−4.21	−5.97
diDIPPBI (**4c**)	702	1.77	−0.62	−4.18	−5.95

2.2. Power conversion efficiency

Once isolated, the diPBIs are soluble in common solvents like chloroform, THF, toluene, and chlorobenzene, and fully soluble at the concentrations for analysis (20 mg/mL in $CDCl_3$ for NMR, and up to

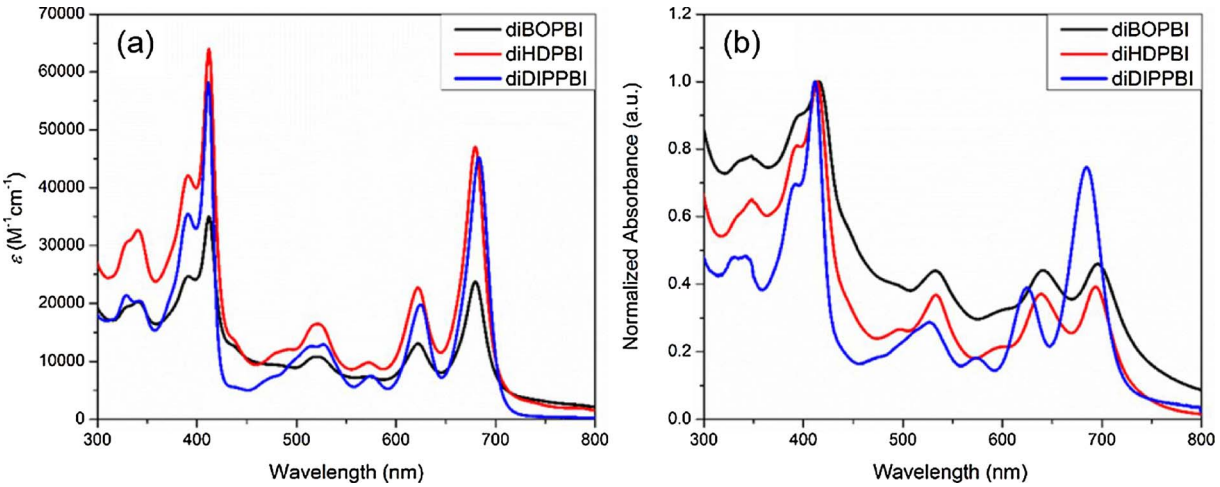

Fig. 2. UV–vis absorption spectra of diPBIs in $CHCl_3$ solution (a) and cast into thin films (b). Similar absorption profiles in solution for each diPBI show that solubilizing group does not have a large impact on the absorption of the molecule, though absorption in the solid state is greatly impacted by choice of aliphatic vs. aryl substituents.

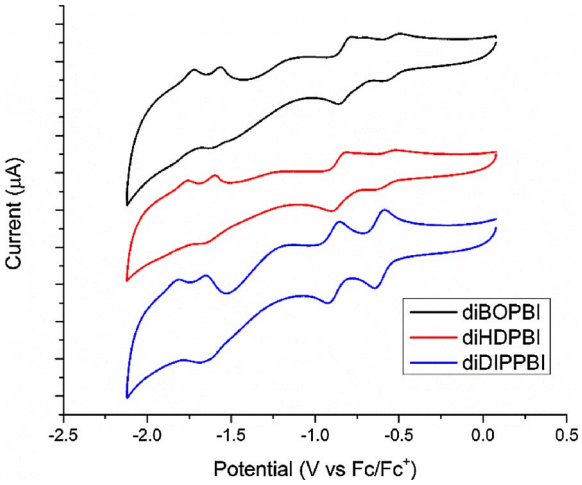

Fig. 3. Reductive cyclic voltammograms of diBOPBI **4a**, diHDPBI **4b**, and diDIPPBI **4c**.

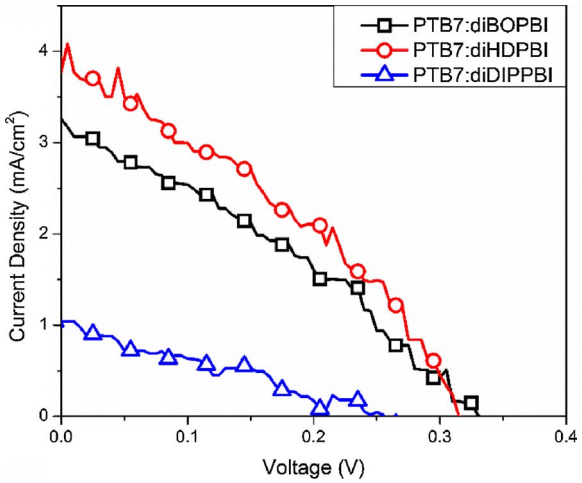

Fig. 4. Representative J–V plots of OPV devices with the architecture ITO/PEDOT:PSS/active layer/Ca/Al utilizing an active layer of 1:1.5 PTB7:diPBI.

9 mg/mL in chlorobenzene). Surprisingly, diDIPPBI was only sparingly soluble in 1,2-dichlorobenzene even upon heating at 60 °C for two hours, so for photovoltaic active layer blends, chlorobenzene was utilized as the casting solvent. Devices were fabricated utilizing PTB7:diPBI blends at differing weight ratios. Representative J–V plots are shown in Fig. 4, and performance parameters are summarized in Table 3. Inverted devices with the architecture ITO/ZnO/active layer/MoO_3/Ag were fabricated and showed no appreciable performance [30,31]. The power conversion efficiencies of the devices are lower than those reported previously for a system that utilized a similar donor polymer and different D:A weight ratios [22]. The open-circuit voltages of these devices are low compared to those reported for other devices based on the donor polymer PTB7 [15,32,33]. This is likely due to multiple factors, like the LUMO level of the diPBIs, which affects values obtainable for the V_{oc} [34], as well as poor connections due to the aggregation of the diPBIs. The report by Jiang et al. that explored the performance of PBI dimers with varying numbers of bay linkages showed that polymer OPV devices based on the triply linked diPBIs showed lower V_{oc}s than devices based on the singly- or doubly-linked dimers, which showed V_{oc} values in accordance with those of devices based on the PBI family as the acceptor [22]. In addition to varied solubility, the LUMOs of the triply-linked diPBIs were lower-lying than those of the singly and doubly linked diPBIs by roughly 0.2 eV. The change in energy levels led to a concomitant drop of similar magnitude in the V_{oc} of resulting devices. The results reported by Jiang et al. for the triply linked materials are similar to those observed in our devices. The short-circuit current densities are also low, especially for **4c**, presumably due to poor charge transport of the acceptor caused by an increased level of π-π stacking in the aryl R-groups, which increases the number of charge traps and limits the number of charge carriers that can escape the phase-separated domains. The highest PCE is observed for the devices utilizing **4b** at the 1:1.5 D:A ratio, driven by the large increase in the J_{sc} under those conditions. In the bulk heterojunction polymer blend configuration of the OPV devices evaluated in the present study, the strong π-stacking of the diPBIs likely leads to self-aggregation, which hinders the formation of an interconnected three-dimensional network.

Solid-state UV–Vis spectra of the PTB7:diPBI films at a 1:1.5 ratio are shown in Fig. 5. All films retained the distinctive diPBI absorption peaks at ~400 nm and ~520 nm. However, in the PTB7:diDIPPBI film, the diPBI absorption peak is dramatically higher than in the alkyl diPBI films, as seen in the neat diDIPPBI film. This is most likely due to formation of large crystalline domains of diDIPPBI, driven by the high aromatic content of these molecules, which results in poor charge separation and generation. This is reflected in the lower PCE of the diDIPPBI devices reported in Table 3.

AFM height images of the 1:1.5 PTB7:diPBI blends in Fig. 6 show small phase-separated crystalline domains consistent with blends of high performance polymers with other acceptors, fullerene and non-fullerene alike [22,35]. The aliphatic-substituted diPBIs in column A and B show phase separation into co-continuous morphologies, which are also seen via phase imaging. The height images in column C, corresponding to the PTB7:diDIPPBI blend, show more discrete phase separation, with round projections from the surface evident in image C2. Phase imaging, though, reveals a stark difference in the phase separation in the films with aliphatic (A3 and B3) vs. aromatic (C3) diPBIs. A3 and B3 show a co-continuous morphology without a great difference in the phase angle, indicating relative homogeneity on the surface. C3 shows a large difference in the phase angle between the bright and dark spots, indicating a high level of phase separation. This is attributed to the diDIPPBI's increased aromatic character, driving π-π stacking and aggregation. RMS roughness analysis of the surfaces shows a rougher surface for the PTB7:diDIPPBI blend ($RMS_{5\mu m}$ = 1.47 nm) than for the PTB7:diBOPBI blend ($RMS_{5\mu m}$ = 1.05 nm) or PTB7:diHDPBI blend ($RMS_{5\mu m}$ = 0.83 nm). For PTB7-based devices, a rougher active layer surface is correlated with decreased performance [36].

Table 3
Performance parameters of PTB7:diPBI devices at varied donor:acceptor weight ratios.

Acceptor	D:A ratio	V_{oc} (V)	J_{sc} (mA/cm^2)	FF (%)	PCE (%)
diBOPBI (**4a**)	1:1	0.350 ± 0.017	3.26 ± 0.22	39.3 ± 4.1	0.45 ± 0.09
	1:1.5	0.335 ± 0.025	3.52 ± 0.21	37.1 ± 5.8	0.43 ± 0.06
diHDPBI (**4b**)	1:1	0.339 ± 0.010	2.57 ± 0.13	46.4 ± 5.2	0.38 ± 0.04
	1:1.5	0.331 ± 0.020	3.79 ± 0.17	39.9 ± 3.6	0.48 ± 0.05
diDIPPBI (**4c**)	1:1	0.281 ± 0.067	0.92 ± 0.12	40.6 ± 12.1	0.09 ± 0.02
	1:1.5	0.282 ± 0.049	0.96 ± 0.13	31.9 ± 4.9	0.08 ± 0.02

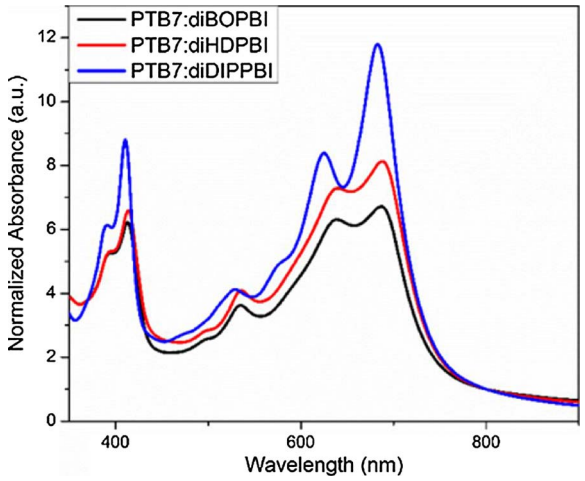

Fig. 5. Solid-state UV–Vis spectra of 1:1.5 PTB7:diPBI films. Absorbance peaks in the diDIPPBI (**4c**) spectrum at 620 and 700 nm show absorbance from the diDIPPBI only, indicating poor charge transfer.

3. Conclusions

A new higher-yielding solvent and ligand system of dimethylacetamide and 2-picolinic acid for monobay dehalogenation of tetrahalogenated PBIs was developed for reactions involving PBIs insoluble in DMSO. The solvent system can also be easily applied to systems that are soluble in DMSO, resulting in higher yields. This establishes a platform for the utilization of a wider array of 1,12-dihalogenated PBIs in electronic material design. Triply-linked perylene bisimide dimers (diPBIs) were synthesized from 1,6,7,12-tetrabromoPBIs in a direct coupling route, in higher overall yields than a route that first required the synthesis and purification of the 1,12-dibromoPBIs. To our knowledge, this is the first report of the direct coupling of aliphatic tetrabromo PBIs to yield triply-linked diPBIs.

The diPBIs were utilized as non-fullerene acceptors in polymer photovoltaic devices. Devices were prepared using PTB7 as the polymer donor material, and demonstrated poor to modest performance compared to devices using similar materials in the active layer. Aliphatic-substituted diPBIs gave PCEs around 0.4%, while the aryl-substituted diPBI gave less than 0.1 %. Many factors influenced the ultimate performance, including the diPBIs' energy-level matching with the donor polymer PTB7. Each diPBI compound exhibited very similar optoelectronic properties, and only differed with the type of solubilizing group.

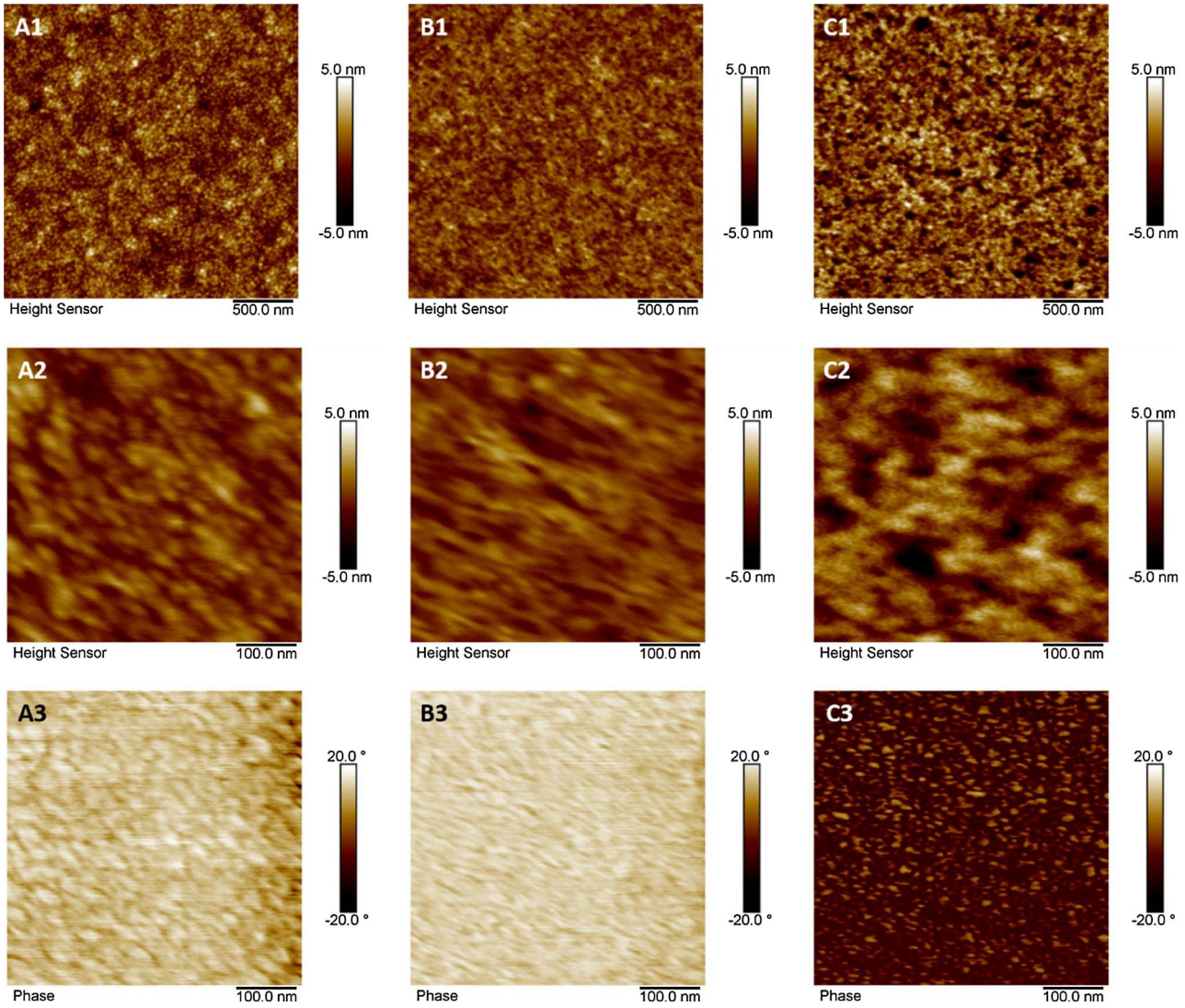

Fig. 6. AFM images of PTB7:diPBI blends at the 1:1.5 wt ratio. Images in column A are PTB7:diBOPBI (**4a**) blends, column B PTB7:diHDPBI (**4b**) blends, and column C PTB7:diDIPPBI (**4c**) blends. Images in row 1 are 2.5 μm × 2.5 μm height images, row 2 are 500 nm × 500 nm height images, and row 3 are 500 nm × 500 nm phase images.

The poorer performance of the aryl diPBI is due to the additional aromatic stacking, leading to crystalline domains that trap charges, limiting performance. The strong π-π stacking of these materials limits their applicability in OPV applications, but the new method for modification of PBIs expands the architectures available for PBI-based molecules and non-fullerene acceptors, providing the potential to tune the composition for specific applications.

4. Experimental section

4.1. Materials

All materials were obtained from Sigma-Aldrich at reagent grade or better unless otherwise stated. Dimethyl acetamide and dimethyl sulfoxide were anhydrous. Solvents for chromatography were obtained from Fisher Scientific and were ACS grade. Silica gel was obtained from Sorbtech, and preparative thin layer chromatography plates (1 mm thick silica) were obtained from AnalTech.

Patterned ITO coated glass substrates with a resistivity of 15 Ω/sq were purchased from Luminescence Technology Corp. Low conductivity grade poly(3,4-ethylenedioxythiophene)-poly(styrenesulfonate) (PEDOT-PSS) was obtained from Sigma Aldrich as a 2.8 wt.% dispersion in water and used as the hole transport layer. PTB7 (80,000–200,000 g/mol, $Đ \leq 3.0$) was obtained from Sigma Aldrich. UV-curable encapsulation epoxy (E131) was obtained from Ossila.

4.2. Analytical techniques

NMR spectra were obtained in $CDCl_3$ on a Varian 300 MHz spectrometer or a Bruker 600 MHz spectrometer and were referenced to the residual solvent peak. MALDI-TOF mass spectra were obtained on a Bruker BioFlex 2, using dithranol as the matrix, and a 20:1 mass ratio of matrix to analyte, cast from THF. These conditions led to fragmentation of the brominated PBIs [37] (Figs. S3, S6, S9, S12, S15, and S18) and mass spectra exhibit a peak consistent with loss of a bromine atom, which are not seen in NMR. Aliphatic diPBIs exhibit a dimeric peak as well (Figs. S20 and S22).

UV–vis spectra of diPBIs (solution-state and thin film) were obtained using a Cary 5000 UV–Vis-NIR spectrophotometer. Spectral normalization was carried out at 800 nm, where there is negligible absorption by the blend components. Solution-state UV–Vis of diPBIs was carried out in dilute solution (1.0×10^{-5} M) in chloroform, and thin films for solid-state UV–Vis were spin-cast from chlorobenzene onto quartz substrates utilizing the same parameters as the active layer. Active layer films for absorption measurements were spin-cast onto quartz substrates, absorption measured with a Perkin-Elmer Lambda 35 UV/Vis spectrophotometer, and AFM imaging was performed on these films on the same day to avoid the detrimental effects of changing ambient conditions, and were conducted on a Dimension ICON scanning probe microscope from Bruker. All the processes were performed in tapping mode in air mode using Nanoscope 8 software. Cyclic voltammetry measurements were performed utilizing a Princeton Applied Research VersaSTAT 4 Potentiostat using Pt working and counter electrodes, with an Ag pseudo-reference electrode. Freshly distilled dichloromethane was used as the solvent, 0.1 M Bu_4NPF_6 as the supporting electrolyte, and the analyte at 0.02 wt%.

4.3. Synthesis of precursors and target compounds

Branched alkylamines (2-butyl-1-octylamine and 2-hexyl-1-decylamine) for the imidization reaction were synthesized from the starting alcohols utilizing the Gabriel synthesis, outlined by Guo et al. [27]. 1,6,7,12-tetrabromoperylene bisanhydride (Br_4PBA, **1**) was synthesized according to Qiu et al. [12].

4.4. N,N'-bis(2-butyl-1-octyl)-1,6,7,12-tetrabromoperylene-3,4,9,10-tetracarboxylic acid bisimide (Br_4BOPBI, **2a**)

Br_4PBA (4.0 g, 5.6 mmol) was weighed into a 250 mL round bottom flask, and 100 mL of propionic acid was added. The suspension was purged with nitrogen and stirred. After 30 min, 2-butyl-1-octylamine (4.15 g, 22.4 mmol) was added, and the temperature was brought to 140 °C and held for 4 h. The majority of propionic acid was subsequently removed via rotary evaporation, and the crude reaction mixture was precipitated into methanol. The solids were collected and purified via silica gel column chromatography with 3:2 toluene/hexanes as the eluent. The fractions were combined, the volume was reduced via rotary evaporation, and the final material was precipitated into methanol, affording 3.33 g (57.1% yield) of Br_4BOPBI as a red solid. ^{1}H NMR (300 MHz, $CDCl_3$): δ 8.83 (s, 4H), 4.15, 4.13 (d, 4H), 1.99 (m, 2H), 1.32 – 1.27 (m, 32H), 0.90 – 0.87 (m, 12H). ^{13}C NMR (75 MHz, $CDCl_3$): δ 162.55, 136.18, 131.64, 131.44, 123.95, 122.66, 44.96, 36.71, 31.88, 31.61, 31.30, 29.73, 28.64, 26.42, 23.11, 22.67, 14.17. Note: some aliphatic peaks overlap. MS (MALDI-TOF) calculated for $[M]^+$: 1042.1, found: 1042.8. ^{1}H NMR, ^{13}C NMR, and MALDI-TOF mass spectra are presented in Figs. S1–S3 in the Supplementary Information.

4.5. N,N'-bis(2-hexyl-1-decyl)-1,6,7,12-tetrabromoperylene-3,4,9,10-tetracarboxylic acid bisimide (Br_4HDPBI, **2b**)

Br_4PBA (4.0 g, 5.6 mmol) was weighed into a 250 mL round bottom flask, 100 mL of propionic acid was added, and the suspension was purged with nitrogen and stirred. After 30 min, 2-hexyl-1-decylamine (5.41 g, 22.4 mmol) was added, and the temperature was brought to 140 °C and held for 4 h. The majority of propionic acid was subsequently removed via rotary evaporation, and the crude reaction mixture was precipitated into methanol. The solids were collected and purified via silica gel column chromatography with 1:1 toluene/hexanes as the eluent. The fractions were combined, the volume was reduced via rotary evaporation, and the mixture was precipitated into methanol, affording 3.77 g (57.8% yield) of Br_4HDPBI as a red solid. ^{1}H NMR (300 MHz, $CDCl_3$): δ 8.83 (s, 4H), 4.15, 4.13 (d, 4H), 1.99 (m, 2H), 1.32 – 1.27 (m, 48H), 0.90 – 0.87 (m, 12H). ^{13}C NMR (75 MHz, $CDCl_3$): δ 162.54, 136.18, 131.63, 131.43, 123.95, 122.66, 44.98, 36.72, 31.89, 31.61, 30.04, 29.72, 29.60, 29.32, 26.43, 22.68, 14.15. Note: some aliphatic peaks overlap. MS (MALDI-TOF) calculated for $[M]^+$: 1154.2, found: 1155.0. ^{1}H NMR, ^{13}C NMR, and MALDI-TOF mass spectra are presented in Figs. S4–S6 in the Supplementary Information.

4.6. N,N'-bis(2,6-Diisopropylphenyl)-1,6,7,12-tetrabromoperylene-3,4,9,10-tetracarboxylic acid bisimide (Br_4DIPPBI, **2c**)

Br_4DIPPBI was synthesized according to the procedure outlined by Qiu et al, and isolated utilizing silica gel column chromatography with toluene as the eluent [12]. ^{1}H NMR (300 MHz, $CDCl_3$): δ 8.92 (s, 4H), 7.56, 7.54, 7.51 (t, 2H), 7.39, 7.37 (d, 4H), 2.76 (m, 4H), 1.21, 1.19 (d, 24H) ^{13}C NMR (75 MHz, $CDCl_3$): δ 162.28, 145.59, 136.60, 132.01, 131.72, 130.04, 129.84, 124.58, 124.28, 122.63, 29.27, 24.07. MS (MALDI-TOF) calculated for $[M]^+$: 1026.0, found: 1026.7. ^{1}H NMR, ^{13}C NMR, and MALDI-TOF mass spectra are presented in Figs. S7–S9 in the Supplementary Information.

4.7. N,N'-bis(2-butyl-1-octyl)-1,12-dibromoperylene-3,4,9,10-tetracarboxylic acid bisimide (Br_2BOPBI, **3a**)

Br_4BOPBI (1.50 g, 1.4 mmol), CuI (1.64 g, 8.4 mmol), and 2-picolinic acid (1.24 g, 9.8 mmol) were weighed into a Schlenk flask, the flask was sealed with a rubber septum, and the system was purged with nitrogen for 30 min. Anhydrous dimethylacetamide (DMAc) (22 mL) was injected into the flask, and the reaction was heated at 75 °C for 6 h. The reaction mixture was allowed to come to room temperature, and

the solution was poured into DI water and stirred for 1 h. The solids were filtered, dried, and purified via silica gel column chromatography with a gradient elution from 1:1 DCM/hexanes to 2:1 DCM/hexanes after elution of unreacted Br_4BOPBI. Br_2BOPBI was isolated as a red solid (616 mg, 48.4% yield). ^{1}H NMR (300 MHz, $CDCl_3$): δ 8.84 (s, 2H), 8.74, 8.71 (d, 2H), 8.57, 8.54 (d, 2H), 4.17, 4.14 (d, 4H), 2.01 (m, 2H), 1.34 – 1.27 (m, 32H), 0.90 – 0.87 (m, 12H). ^{13}C NMR (75 MHz, $CDCl_3$): δ 163.39, 162.87, 137.28, 134.43, 132.58, 130.69, 129.34, 126.88, 124.03, 123.40, 123.23, 122.78, 44.81, 36.67, 31.87, 31.64, 31.33, 29.74, 28.65, 26.46, 23.10, 22.67, 14.15. Note: some aliphatic peaks overlap. MS (MALDI-TOF) calculated for $[M]^+$: 884.3, found: 884.8. ^{1}H NMR, ^{13}C NMR, and MALDI-TOF mass spectra are presented in Figs. S10– S12 in the Supplementary Information.

Alternatively, Br_4BOPBI (500 mg, 0.48 mmol), CuI (548.5 mg, 2.88 mmol), L-proline (386.8 mg, 3.36 mmol), and diphenyl sulfoxide (2.1 g) were weighed into a Schlenk flask and purged with nitrogen for 30 min. Anhydrous DMSO (5.8 mL) was injected into the flask, and the reaction was heated at 75 °C for 6 h, the flask was allowed to cool to room temperature, and the reaction mixture was poured into methanol. The products were purified using the same method as for the previous system (99.4 mg, 23.4% yield).

4.8. N,N'-bis(2-hexyl-1-decyl)-1,12-dibromoperylene-3,4,9,10-tetracarboxylic acid bisimide (Br_2HDPBI, **3b**)

Br_4HDPBI (2.31 g, 2.0 mmol), CuI (2.29 g, 12.0 mmol), and 2-picolinic acid (1.72 g, 14.0 mmol) were weighed into a Schlenk flask, the flask was sealed with a rubber septum, and the system was purged with nitrogen for 30 min. Anhydrous dimethylacetamide (DMAc) (30 mL) was injected into the flask, and the reaction was heated at 75 °C for 6 h. The reaction mixture was allowed to come to room temperature, and the solution was poured into DI water and stirred for 1 h. The solids were filtered, dried, and purified via silica gel column chromatography with a gradient elution from 1:1 DCM/hexanes to 2:1 DCM/hexanes after elution of unreacted Br_4HDPBI. Br_2HDPBI was isolated as a red solid (924 mg, 46.4% yield). 1H NMR (300 MHz, $CDCl_3$): δ 8.83 (s, 2H), 8.72, 8.70 (d, 2H), 8.56, 8.53 (d, 2H), 4.17, 4.14 (d, 4H), 1.99 (m, 2H), 1.32 – 1.24 (m, 48H), 0.90 – 0.87 (m, 12H). ^{13}C NMR (75 MHz, $CDCl_3$): δ 163.56, 162.84, 137.27, 134.40, 132.56, 130.67, 129.31, 126.86, 124.02, 123.37, 123.23, 122.77, 44.85, 36.69, 31.90, 31.67, 30.05, 29.74, 29.60, 29.32, 26.48, 23.10, 14.14. Note: some aliphatic peaks overlap. MS (MALDI-TOF) calculated for $[M]^+$: 996.4, found 997.1. ^{1}H NMR, ^{13}C NMR, and MALDI-TOF mass spectra are presented in Figs. S13–S15 in the Supplementary Information.

Alternatively, Br_4HDPBI (500 mg, 0.43 mmol), CuI (494.8 mg, 2.58 mmol), L-proline (349.0 mg, 3.03 mmol), and diphenyl sulfoxide (1.9 g) were weighed into a Schlenk flask and purged with nitrogen for 30 min. Anhydrous DMSO (5.3 mL) was injected into the flask, and the reaction mixture was heated at 75 °C for 6 h, allowed to cool to room temperature, and poured into methanol. The products were purified using the same method as for the previous system (85.9 mg, 19.9% yield).

4.9. N,N'-bis(2,6-Diisopropylphenyl)-1,12-dibromoperylene-3,4,9,10-tetracarboxylic acid bisimide (Br_2DIPPBI, **3c**)

Br_4DIPPBI (500 mg, 0.49 mmol), CuI (558 mg, 2.93 mmol), and 2-picolinic acid (421 mg, 3.42 mmol) were weighed into a Schlenk flask, the flask was sealed with a rubber septum, and the system was purged with nitrogen for 30 min. Anhydrous dimethylacetamide (DMAc) (7.3 mL) was injected into the flask, and the reaction was heated at 75 °C for 6 h. The reaction mixture was allowed to come to room temperature, and the solution was poured into DI water and stirred for 1 h. The solids were filtered, dried, and purified via silica gel column chromatography with a gradient elution from 1:1 DCM/hexanes to 2:1 DCM/hexanes after elution of unreacted Br_4DIPPBI. Br_2DIPPBI was isolated as a red solid (213 mg, 50.4% yield). ^{1}H NMR (300 MHz, $CDCl_3$) δ 8.86 (s, 2H), 8.77, 8.74 (d, 2H), 8.59, 8.57 (d, 2H), 7.48, 7.46, 7.43 (t, 2H), 7.31, 7.29 (d, 4H), 2.70 (m, 4H), 1.12 (m, 24H). ^{13}C NMR (75 MHz, $CDCl_3$) δ 163.31, 162.62, 145.59, 137.68, 134.83, 133.00, 131.49, 131.29, 130.14, 129.89, 129.65, 127.55, 124.20, 123.67, 123.24, 122.83, 29.22, 24.02. MS (MALDI-TOF) calculated for $[M]^+$: 868.1, found 868.0. ^{1}H NMR, ^{13}C NMR, and MALDI-TOF mass spectra are presented in Figs. S16–S18 in the Supplementary Information.

Alternatively, Br_4DIPPBI (500 mg, 0.49 mmol), CuI (558 mg, 2.93 mmol), and L-proline (393 mg, 3.42 mmol) were weighed into a Schlenk flask and purged with nitrogen for 30 min. Anhydrous DMSO (7.3 mL) was injected into the flask, and the reaction mixture was heated at 75 °C for 6 h, allowed to cool to room temperature, and poured into methanol. The products were purified using the same method as for the previous system (95.2 mg, 22.5% yield).

4.10. Di(butyloctyl perylene bisimide), diBOPBI, **4a**

Br_2BOPBI (575 mg, 0.65 mmol), CuI (743 mg, 3.90 mmol), L-proline (524 mg, 4.55 mmol), potassium carbonate (898 mg, 6.50 mmol), and phenyl sulfoxide (2.6 g) were weighed into a Schlenk flask. The solids were purged with nitrogen for 45 min, after which anhydrous DMSO (7 mL) was injected. The reaction mixture was heated at 110 °C for 12 h. After cooling to room temperature, the reaction mixture was poured into 1 M HCl in methanol and allowed to stir for 1 h. The solids were filtered off, collected, and purified via silica column chromatography using 3:2 DCM/hexanes to 1:1 DCM/hexanes. The fractions with the target compound were then purified via preparatory TLC with 3:2 toluene/DCM as the eluent. The product was then scraped off of the plate and eluted from the silica with DCM and methanol, affording the 54.3 mg of the product (11.5% yield) as a black-blue solid. ^{1}H NMR (600 MHz, $CDCl_3$): δ 9.41 – 8.70 (m, 10H), 4.47 – 4.14 (m, 8H), 2.17 – 2.06 (m, 4H), 1.40 – 0.67 (m, 88H). ^{13}C NMR spectra were not well-resolved. MS (MALDI-TOF) calculated for $[M]^+$ 1447.8, found 1448.0. ^{1}H NMR and MALDI-TOF mass spectra are presented in Figs. S19 and S20 in the Supplementary Information.

Alternatively, Br_4BOPBI (500 mg, 0.48 mmol), CuI (549 mg, 2.88 mmol), L-proline (387 mg, 3.36 mmol), potassium carbonate (663.4 mg, 4.80 mmol), and phenyl sulfoxide (2.1 g) were weighed into a Schlenk flask, purged with nitrogen for 45 min, and 5.8 mL DMSO was injected via syringe. The reaction mixture was subjected to the same conditions as the above procedure yielding diBOPBI (35.7 mg, 10.3% yield).

4.11. Di(hexyldecyl perylene bisimide), diHDPBI, **4b**

Br_2HDPBI (750 mg, 0.75 mmol), L-proline (609 mg, 5.25 mmol), CuI (863 mg, 4.5 mmol), K_2CO_3 (1.044 g, 7.5 mmol), and phenyl sulfoxide (2.4 g) were weighed into a Schlenk flask, the flask was sealed with a rubber septum, and the reaction mixture was purged with nitrogen for 45 minutes. Anhydrous DMSO (7.3 mL) was added via a syringe, and the reaction was heated at 110 °C for 12 h. The reaction mixture was brought to room temperature and poured into 1M HCl in methanol and stirred for 1 h. The solids were isolated by filtration and redissolved into DCM. The target compound was isolated via silica gel column chromatography via gradient elution from 3:2 DCM/hexanes to 1:1 DCM/hexanes to remove the impurities that travel quickly. The fractions with the target compound were then purified via preparatory TLC with 3:2 toluene/DCM as the eluent. The final product was eluted from the silica with DCM and methanol affording 111.3 mg of the product (17.6% yield) as a black-blue solid. 1H NMR (600 MHz, $CDCl_3$): δ 9.46 – 8.73 (m, 10H), 4.50 – 4.17 (m, 8H), 2.20 – 2.05 (m, 4H), 1.40 – 0.69 (m, 120H). ^{13}C NMR spectra were not well resolved.MS (MALDI-TOF) calculated for $[M]^+$: 1672.1, found 1672.3. ^{1}H NMR and MALDI-TOF mass spectra are presented in Figs. S21 and S22 in the Supplementary Information.

Alternatively, Br_4HDPBI (500 mg, 0.43 mmol), L-proline (349 mg, 3.0 mmol), CuI (495 mg, 2.6 mmol), K_2CO_3 (598 g, 4.3 mmol), and phenyl sulfoxide (1.9 g) were weighed into a Schlenk flask, purged with nitrogen for 45 min, and 5.3 mL DMSO was injected via syringe. The reaction mixture was subjected to the same conditions as the above procedure yielding diHDPBI (35.9 mg, 9.9% yield).

4.12. Di(diisopropylphenyl perylenebisimide), diDIPPBI, **4c**

Compound **4c** was synthesized according to the previous report by Qian et al., and isolated at a 24.6% yield. ^{1}H NMR and MALDI-TOF mass spectra are in agreement with literature [21]. ^{1}H NMR and MALDI-TOF mass spectra are presented in Figs. S23 and S24 in the Supplementary Information.

4.13. Device fabrication for determination of power conversion efficiency

PTB7 and the respective diPBIs were weighed into an amber vial in a nitrogen-filled glovebox at the desired weight ratio. Chlorobenzene was added to bring the total concentration to 15 mg/mL, and the mixture was heated at 60 °C for 8 h in the glovebox. ITO-coated glass substrates (Lumtech) were successively cleaned ultrasonically in deionized water, acetone, and isopropanol for ten minutes each. They were dried under flowing nitrogen and exposed to UV/ozone for 40 min in a ProCleaner™ Plus system, after which a layer of PEDOT:PSS was spin coated at a speed of 5000 rpm for one minute. The PEDOT:PSS-coated substrates were baked on a hotplate at 150 °C for ten minutes and transferred to a nitrogen-filled glovebox. The active layer was then spin-coated at 1250 rpm for 70 s, giving an active layer thickness around 100 nm, as measured by AFM scratch testing. The devices were then transferred in a shadow mask into an Angstrom Engineering thermal evaporator system, and a vacuum was applied at 10^{-6} torr. Layers of calcium (20 nm) and aluminum (80 nm) were subsequently deposited at 1 Å/s. The devices were encapsulated with UV-curable epoxy (Ossila) and a glass cover slip and were transferred outside the glovebox to immediately cure the epoxy by exposure to UV irradiation for six minutes. The devices were then immediately tested. Current-voltage (J–V) measurements were carried out with a Keithley 2400 source unit coupled to an AM1.5 Photo Emission Tech solar simulator, with illumination of 1000 W/m^2 from a xenon lamp coupled to a monochromator. For each experimental material, four identical devices were fabricated, each having six pixels, with active areas of 0.042 cm^2. The top-performing 75% of pixels were used for statistical analysis.

Acknowledgements

This work was supported in part by the Department of Education Graduate Assistance in Areas of National Need (GAANN) Award# P200A120118, and by a fellowship through the National Science Foundation NRT *INTERFACE* Award#1449999 through the University of Southern Mississippi. Partial support through NSF OIA-1632825 is acknowledged. Special thanks are given to Dr. Evgueni Nesterov and his research group at Louisiana State University for use of their device fabrication facilities, and to James Brownlow and Turkesa Bullock from Hattiesburg High School for their help through the National Science Foundation Research Experience for Teachers (RET) in Engineering and Computer Science Site for Sustainable Polymer Engineering Research Award # EEC-1406753.

Appendix A. Supplementary data

Supplementary material related to this article can be found, in the online version, at doi:https://doi.org/10.1016/j.synthmet.2018.02.005.

References

[1] C.B. Nielsen, S. Holliday, H.-Y. Chen, S.J. Cryer, I. McCulloch, Non-fullerene electron acceptors for use in organic solar cells, Acc. Chem. Res. 48 (11) (2015) 2803–2812.
[2] Y. Lin, F. Zhao, Q. He, L. Huo, Y. Wu, T.C. Parker, W. Ma, Y. Sun, C. Wang, D. Zhu, A.J. Heeger, S.R. Marder, X. Zhan, High-performance electron acceptor with thienyl side chains for organic photovoltaics, J. Am. Chem. Soc. 138 (14) (2016) 4955–4961.
[3] Aa.F. Eftaiha, J.-P. Sun, I.G. Hill, G.C. Welch, Recent advances of non-fullerene, small molecular acceptors for solution processed bulk heterojunction solar cells, J. Mater. Chem. A 2 (5) (2014) 1201–1213.
[4] C.W. Tang, Two-layer organic photovoltaic cell, Appl. Phys. Lett. 48 (2) (1986) 183–185.
[5] H. Dong, X. Fu, J. Liu, Z. Wang, W. Hu, 25th anniversary article: key points for high-mobility organic field-effect transistors, Adv. Mater. (Weinheim, Ger.) 25 (43) (2013) 6158–6183.
[6] A. Lv, S.R. Puniredd, J. Zhang, Z. Li, H. Zhu, W. Jiang, H. Dong, Y. He, L. Jiang, Y. Li, W. Pisula, Q. Meng, W. Hu, Z. Wang, High mobility, air stable, organic single crystal transistors of an n-type diperylene bisimide, Adv. Mater. (Weinheim, Ger.) 24 (19) (2012) 2626–2630.
[7] Z. Liu, Y. Wu, Q. Zhang, X. Gao, Non-fullerene small molecule acceptors based on perylene diimides, J. Mater. Chem. A 4 (45) (2016) 17604–17622.
[8] Y. Lin, Y. Wang, J. Wang, J. Hou, Y. Li, D. Zhu, X. Zhan, A star-shaped perylene diimide electron acceptor for high-performance organic solar cells, Adv. Mater. 26 (30) (2014) 5137–5142.
[9] E. Kozma, M. Catellani, Perylene diimides based materials for organic solar cells, Dyes Pigm. 98 (1) (2013) 160–179.
[10] L. Yang, Y. Chen, S. Chen, T. Dong, W. Deng, L. Lv, S. Yang, H. Yan, H. Huang, Achieving high performance non-fullerene organic solar cells through tuning the numbers of electron deficient building blocks of molecular acceptors, J. Power Sources 324 (Supplement C) (2016) 538–546.
[11] J.-P. Sun, A.D. Hendsbee, A.J. Dobson, G.C. Welch, I.G. Hill, Perylene diimide based all small-molecule organic solar cells: impact of branched-alkyl side chains on solubility, photophysics, self-assembly, and photovoltaic parameters, Org. Electron. 35 (2016) 151–157.
[12] W. Qiu, S. Chen, X. Sun, Y. Liu, D. Zhu, Suzuki coupling reaction of 1,6,7,12-tetrabromoperylene bisimide, Org. Lett. 8 (5) (2006) 867–870.
[13] J. Zhang, L. Tan, W. Jiang, W. Hu, Z. Wang, N-alkyl substituted di(perylene bisimides) as air-stable electron transport materials for solution-processible thin-film transistors with enhanced performance, J. Mater. Chem. C 1 (19) (2013) 3200–3206.
[14] H. Qian, W. Yue, Y. Zhen, S. Di Motta, E. Di Donato, F. Negri, J. Qu, W. Xu, D. Zhu, Z. Wang, Heterocyclic annelated di(perylene bisimide): constructing bowl-shaped perylene bisimides by the combination of steric congestion and ring strain, J. Org. Chem. 74 (16) (2009) 6275–6282.
[15] Y. Zhong, M.T. Trinh, R. Chen, W. Wang, P.P. Khlyabich, B. Kumar, Q. Xu, C.-Y. Nam, M.Y. Sfeir, C. Black, M.L. Steigerwald, Y.-L. Loo, S. Xiao, F. Ng, X.Y. Zhu, C. Nuckolls, Efficient organic solar cells with helical perylene diimide electron acceptors, J. Am. Chem. Soc. 136 (43) (2014) 15215–15221.
[16] C. Sambiagio, S.P. Marsden, A.J. Blacker, P.C. McGowan, Copper catalysed ullmann type chemistry: from mechanistic aspects to modern development, Chem. Soc. Rev. 43 (10) (2014) 3525–3550.
[17] H. Lin, D. Sun, Recent synthetic developments and applications of the Ullmann reaction. A review, Org. Prep. Proced. Int. 45 (5) (2013) 341–394.
[18] D. Ma, Q. Cai, Copper/amino acid catalyzed cross-couplings of aryl and vinyl halides with nucleophiles, Acc. Chem. Res. 41 (11) (2008) 1450–1460.
[19] X. Xie, G. Cai, D. Ma, Cui/L-proline-catalyzed coupling reactions of aryl halides with activated methylene compounds, Org. Lett. 7 (21) (2005) 4693–4695.
[20] G. Zhang, X. Han, Y. Luan, Y. Wang, X. Wen, C. Ding, L-proline: an efficient N,O-bidentate ligand for copper-catalyzed aerobic oxidation of primary and secondary benzylic alcohols at room temperature, Chem. Commun. 49 (72) (2013) 7908–7910.
[21] H. Qian, F. Negri, C. Wang, Z. Wang, Fully conjugated tri(perylene bisimides): an approach to the construction of n-type graphene nanoribbons, J. Am. Chem. Soc. 130 (52) (2008) 17970–17976.
[22] W. Jiang, L. Ye, X. Li, C. Xiao, F. Tan, W. Zhao, J. Hou, Z. Wang, Bay-linked perylene bisimides as promising non-fullerene acceptors for organic solar cells, Chem. Commun. 50 (2014) 1024–1026.
[23] W. Jiang, C. Xiao, L. Hao, Z. Wang, H. Ceymann, C. Lambert, S. Di Motta, F. Negri, Localization/delocalization of charges in bay-linked perylene bisimides, Chem. Eur. J. 18 (22) (2012) 6764–6775 S6764/1–S6764/24.
[24] Y. Zhen, H. Qian, J. Xiang, J. Qu, Z. Wang, Highly regiospecific synthetic approach to monobay-functionalized perylene bisimide and di(perylene bisimide), Org. Lett. 11 (14) (2009) 3084–3087.
[25] D. Sun, D. Meng, Y. Cai, B. Fan, Y. Li, W. Jiang, L. Huo, Y. Sun, Z. Wang, Non-fullerene-acceptor-based bulk-heterojunction organic solar cells with efficiency over 7%, J. Am. Chem. Soc. 137 (34) (2015) 11156–11162.
[26] B. Pagoaga, L. Giraudet, N. Hoffmann, Synthesis and characterisation of 1,7-di- and inherently chiral 1,12-di- and 1,6,7,12-tetraarylperylenetetracarbox-3,4:9,10-diimides, Eur. J. Org. Chem. 2014 (24) (2014) 5178–5195.
[27] X. Guo, M.D. Watson, Conjugated polymers from naphthalene bisimide, Org. Lett. 10 (23) (2008) 5333–5336.
[28] H. Qian, Z. Wang, W. Yue, D. Zhu, Exceptional coupling of tetrachloroperylene bisimide: combination of Ullmann reaction and C-H transformation, J. Am. Chem.

Soc. 129 (35) (2007) 10664–10665.
[29] C. Zeng, C. Xiao, R. Xin, W. Jiang, Y. Wang, Z. Wang, Influence of alkyl chain branching point on the electron transport properties of di(perylene diimides) thin film transistors, RSC Adv. 6 (2016) 55946–55952.
[30] Y. Sun, J.H. Seo, C.J. Takacs, J. Seifter, A.J. Heeger, Inverted polymer solar cells integrated with a low-temperature-annealed sol-gel-derived Zno film as an electron transport layer, Adv. Mater. 23 (14) (2011) 1679–1683.
[31] S.V. Dayneko, A.D. Hendsbee, G.C. Welch, Fullerene-free polymer solar cells processed from non-halogenated solvents in air with Pce of 4.8%, Chem. Commun. 53 (6) (2017) 1164–1167.
[32] Y. Liang, D. Feng, Y. Wu, S.-T. Tsai, G. Li, C. Ray, L. Yu, Highly efficient solar cell polymers developed via fine-tuning of structural and electronic properties, J. Am. Chem. Soc. 131 (22) (2009) 7792–7799.
[33] B. Ebenhoch, N.B.A. Prasetya, V.M. Rotello, G. Cooke, I.D.W. Samuel, Solution-processed boron subphthalocyanine derivatives as acceptors for organic bulk-heterojunction solar cells, J. Mater. Chem. A 3 (14) (2015) 7345–7352.
[34] M.C. Scharber, D. Mühlbacher, M. Koppe, P. Denk, C. Waldauf, A.J. Heeger, C.J. Brabec, Design rules for donors in bulk-heterojunction solar cells—towards 10 % energy-conversion efficiency, Adv. Mater. 18 (6) (2006) 789–794.
[35] C.H. To, A. Ng, Q. Dong, A.B. Djurišić, J.A. Zapien, W.K. Chan, C. Surya, Effect of Ptb7 properties on the performance of Ptb7:Pc71bm solar cells, ACS Appl. Mater. Interfaces 7 (24) (2015) 13198–13207.
[36] Z. Ding, J. Kettle, M. Horie, S.W. Chang, G.C. Smith, A.I. Shames, E.A. Katz, Efficient solar cells are more stable: the impact of polymer molecular weight on performance of organic photovoltaics, J. Mater. Chem. A 4 (19) (2016) 7274–7280.
[37] E. de Hoffmann, V. Stroobant (Eds.), Mass Spectrometry: Principles and Applications, third edition, John Wiley & Sons, Ltd., 2007, p. p 489.